This is a peer-reviewed, accepted author manuscript of the following research article: Wu, Y, Fan, X, Xu, L, Lu, W & Chen, C 2024, 'A new on-line diagnosis method for inter-turn short circuit of hydro-generator rotor windings using a flexible equivalent coil', IEEE Transactions on Energy Conversion, pp. 1-11. https://doi.org/10.1109/tec.2024.3420879

A new on-line diagnosis method for inter-turn short circuit of hydro-generator rotor windings using a flexible equivalent coil

Yucai Wu. Xuanjie Fan. Lie Xu. Weifu Lu. Cong Chen

***Abstract*—The inter-turn short-circuit(ITSC) fault of hydro-generator rotor windings will lead to the asymmetry of the main magnetic field, which may cause strong vibration and result in a shutdown accident. Inspired by the existence of large number of cross-core screws in hydro-generators, two screws with fractional or integral multiples of generator polar distance are selected and used to form an equivalent coil, so as to construct a semi-intrusive fault detection sensor layout scheme. The theoretical analysis of our method was conducted and real time ITSC fault detection according to specific harmonics in the induced voltage in the equivalent coil was proved to be feasible. Finally, through the finite element simulation and fault simulation test, it is shown that when the ITSC of hydro-generator rotor winding occurs, the fractional harmonics appear in the induced voltage of the equivalent coil, which proves the effectivity of our method in determining the ITSC fault. The signal acquisition by using our method is convenient. Besides, the coil pitch is flexible, which is beneficial for both signal acquisition and feature highlighting.**

***Index Terms*—hydro-generator, rotor winding, inter-turn short-circuit, equivalent coil, harmonic, diagnosis.**

I. Introduction

For large capacity synchronous generators, ITSC of rotor windings is undoubtedly a kind of troublesome fault. The accompanied vibration, winding grounding, bearing electrical corrosion, shaft magnetization and other issues have brought great trouble. Specially, the continuously increasing vibration [1,2] is an important cause of shutdown accident. Due to the diversity of vibration inducements, maintenance staff need to spend a lot of time to determine the cause of vibration, and the cost of long-term shutdown is rather high [3-5]. Therefore, the on-line diagnosis and real-time warning of ITSC fault of rotor windings is extremely necessary and has aroused much attention.

This work was supported by National Natural Science Foundation of China under Grant 52277048 and Natural Science Foundation of Hebei Province under Grant E2023502002. (*Corresponding author: Yucai Wu.*)

Y. Wu and X. Fan are with Hebei Key Laboratory of Green and Efficient New Electrical Materials and Equipment, Department of Electrical Engineering, North China Electric Power University, Baoding 071003, China (e-mail: 51351855@ncepu.edu.cn; fanxuanjie@ncepu.edu.cn;).

L. Xu is with Department of Electronic and Electrical Engineering, University of Strathclyde, Glasgow G1 1XW, UK (e-mail: lie.xu@strath.ac.uk).

W. Lu is with Pumped-storage Technological & Economic Research Institute, State Grid Xinyuan Company LTD., Beijing 100761, China (e-mail: weifu-lu@sgxy.sgcc.com.cn).

C. Chen is with China Power Huachuang(Suzhou) Electricity Technology Research Co., Ltd., Suzhou 215123, China (e-mail: crcn2007@qq.com).

In the field of on-line detection of ITSC fault of synchronous generator rotor winding, the diagnosis method based on macroscopic parameters is difficult to be applied to hydro-generators, such as the excitation current method [6,7], the virtual power method [8], the expected electromotive force method [9]. As hydro-generators have more magnetic poles, ITSC in one magnetic pole has a milder impact on these parameters.

In view of this, researchers have explored other on-line detection methods for ITSC of hydro-generator rotor windings. In [10], the authors proposed to fix a search coil inside the generator, and the ITSC fault of the rotor winding is judged by observing the changes of the tangential magnetic flux and the induced voltage measured by the coil. The coil used in this method has a small diameter and does not need to be disassembled. In [11], a large pitch coil was installed in the stator slot of the generator, and the ITSC fault of rotor winding is judged by the coil induced voltage harmonics. In [12,13], the authors used the asymmetry of the main magnetic field of the generator caused by the short circuit and the asymmetry of the induced electromotive force of the stator winding in the same phase double branch, and proposed to judge the ITSC fault of the rotor winding by the difference of the current of the same phase double branch (2 times of the circulating current). In [14-17], a carbon brush was installed on the excitation side of the generator to make it cooperate with the ground carbon brush on the steam side, and judged the ITSC fault of the rotor winding by the voltage harmonic change between the carbon brushes on both sides. In [18], a method using U-type detection coil was proposed. To obtain the asymmetric characteristics of the main magnetic field of the hydro-generator, the induced voltage of the U-type coil wrapped around the stator core was used to evaluate the asymmetry degree of the rotor magnetic field of the synchronous motor caused by the short circuit failure. According to relevant analysis, it can be concluded that the magnetic field asymmetry can be used to reflect the ITSC fault. In this method, the sensor was arranged inside the motor to get better detection effect. In fact, it is easier to install these coils for newly manufactured units at the factory stage. For some old power plants, people are not very keen on adding coils to their units for involved safety responsibility between the plants and manufacturers, which may cause some dispute. In [19], the authors proposed to install two Hall Effect sensors in the air gap of the hydro-generator. The ITSC of rotor windings fault can be judged by analyzing the sum of the magnetic flux

of the two sensors and the frequency spectral characteristics, and the finite element results were verified on a 100 kVA hydro-generator. In [20], a non-invasive sensor was used to acquire the stray magnetic field signals of the hydro-generator. The time-frequency domain characteristics of the rotor winding ITSC signals were analyzed after short-time Fourier decomposition, and the effectiveness of the method was verified by test data. To improve the sensitivity of fault detection, the sensor usually has many turns, which makes it vulnerable to electromagnetic interference. Therefore, it needs to be further optimized to improve its practicability in the field.

In [21], the authors proposed to install detection coils in the stator slots of different regions of the hydro-generator. By measuring the induced voltage difference of the detection coils, the ITSC fault of the rotor winding of the unit can be detected online, and the position of the fault pole can be located. In [22], a method using the symmetry of the air gap magnetic field of the hydro-generator, and proposed to install two inductive probes on the stator teeth at different positions. The algebraic sum of the induced voltage of the two probes was used to identify the ITSC fault of the rotor winding, which proved the effectiveness of the double probe detection method. In [23], the authors proposed to directly introduce an artificial short-circuit device into the rotor of a 330 MW hydro-generator, and install coils on the surface of the stator teeth to measure the air-gap flux, and detect the ITSC fault of the hydro-generator rotor winding through the change of the peak voltage of the coil at the leading edge of the magnetic pole. In [24], a stray flux probe was proposed to install on the stator core of a hydro-generator, and use the spectral variation characteristics of the stray flux to detect the ITSC fault of the rotor winding.In [25], the time domain or frequency domain characteristics of the induced voltage at the two ends of a cross-core screw in the stator core were used to determine the ITSC fault of hydro-generators rotor winding, which provides a new idea for on-line rotor winding ITSC fault detection. This method does not need to install sensors inside the unit and only utilizes the existing components. It makes the signal acquisition easier compared with invasive detection methods. In addition, the cross-core screws are inside the stator yoke, located in the main magnetic field, so this method also achieves better measurement accuracy and is suitable for both hydro-generators and turbo-generators as synchronous generators are generally equipped with cross-core screws. On the other, this single screw detection method also has some downsides. For example, for large generators, the cross-core screws are usually several meters long, and the measuring leads need to cross the whole axial length of the generator. For vertical hydro-generators, the measuring leads need to pass through the foundation to converge, which is not easy. Besides, the large output voltage needs lowering so as to be collected by the acquisition instrument, which also increases the complexity of the whole acquisition system.

In this paper, we connect any two cross-core screws in a hydro-generator on one side of the generator to form a single-turn coil with adjustable pitch. According to analysis on the magnetic field characteristic of the hydro-generator before and after ITSC, the variation of the induced voltage of the equivalent coil is predicted. Finally, the finite element simulation and fault simulation test verify that the detection coil can effectively detect the ITSC fault of the rotor winding.

II. Analysis on Fault Magnetic Field Characteridtics

For a hydro-generator, once ITSC of rotor windings happen, the effective ampere turns of the fault magnetic pole will decrease and its magnetic potential waveform will change, as shown in Fig. 1.

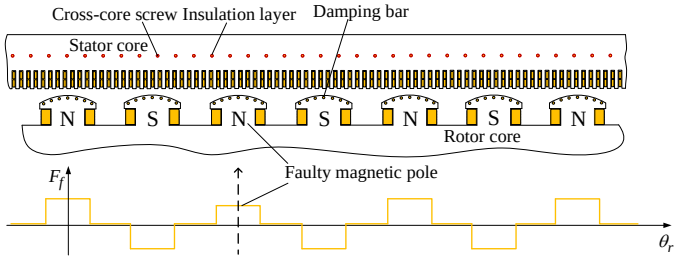

Fig.1. Excitation magnetic field distribution of salient pole synchronous generator.

Accrding to Fig. 1, the magnetic potential on both sides of the fault pole is symmetrical. In view of this, we can move the longitudinal coordinate-axis to the center of the fault pole, and then the excitation magnetic potential after the failure is as follows,

$$\begin{aligned} F_{\text{f.fault}}(\theta_{\text{r}}) &= F_{\text{f.normal}}(\theta_{\text{r}}) + \Delta F_{\text{f}}(\theta_{\text{r}}) \\ &= \sum_{k} F_k \cos kp\theta_{\text{r}} - \Delta F_{\text{f}j} \cos j\theta_{\text{r}} \end{aligned} \tag{1}$$

where, p is the pole-pair number of the hydro-generator, and θ_{r} is the rotor space mechanical angle. Here, k=1, 3, 5,…, n, and j=1, 2, 3,…, n.

For hydro-generators,

$$F_k = \frac{2}{k\pi} I_{\text{f}} N \sin\left(\frac{k\pi}{2}\right) \tag{2}$$

where, I_{f} is the generator excitation current, and N is the turn number of the excitation winding per pole.

Through Fourier decomposition, the magnetic potential generated by the short-circuited winding with the same excitation current in the reverse direction can be expressed as follows [26],

$$\Delta F_{\text{f}}(\theta_{\text{r}}) = -\sum_{k=1,2,3,\cdots,n} \left[F_{k_1} \cos(k\theta_{\text{r}}) + F_{k_2} \sin(k\theta_{\text{r}}) \right] \tag{3}$$

$$\begin{aligned} F_{k_1} &= \frac{1}{p\pi} \int_0^{2p\pi} F_{\text{f}}(\theta_{\text{r}}) \cos(k\theta_{\text{r}}) \, \mathrm{d}p\theta_{\text{r}} \\ &= \frac{iw'}{p\pi} \frac{\sin(2pk\pi)}{2pk} \end{aligned} \tag{4}$$

$$\begin{aligned} F_{k_2} &= \frac{1}{p\pi} \int_0^{2p\pi} F_{\text{f}}(\theta_{\text{r}}) \sin(k\theta_{\text{r}}) \, \mathrm{d}p\theta_{\text{r}} \\ &= \frac{iw'}{p\pi} \frac{\left[2p\cos(k\pi) - \cos(2pk\pi) - (2p-1) \right]}{2pk} \end{aligned} \tag{5}$$

where, w' is the turn number of the short-circuited coil.

When ITSC of rotor windings occurs, the excitation magnetic potential of the hydro-generator can be expressed as follows,

$$F(\theta_r)=\sum_{k=1,3,5,\cdots,n}F_k\cos(kp\theta_r)-\sum_{k=1,2,3,\cdots,n}\left[F_{k_1}\cos(k\theta_r)+F_{k_2}\sin(k\theta_r)\right] \tag{6}$$

After failure, the k/p^{th} harmonic magnetic potential appears in the air gap due to the influence of excitation magnetic potential increment ΔF_f, which does not exist when the rotor winding is normal.

The correlation between the magnetic flux density and magnetic potential is as follows,

$$F\lambda=B \tag{7}$$

where, F is the magnetic potential; for a uniform magnetic circuit, the permeance per unit area $\lambda = \mu/l$, referred as the permeability coefficient; l is the length of magnetic circuit; μ is the permeability; B is the magnetic flux density.

The established coordinate axis (d axis) is located in the center of the magnetic pole, considering the dynamic eccentricity of the rotor, the air gap permeance can be expressed as follows,

$$\lambda(\theta_r)=\frac{\lambda_0}{2}+\sum_l\lambda_{2l}\cos 2lp\theta_r+\sum_j\lambda_j\cos j(\theta_r+\varphi_{dj}) \tag{8}$$

where, λ_0 is a constant, λ_{2l} is the $2l^{th}$ harmonic amplitude of air gap permeance, λ_j is the j/p^{th} harmonic amplitude of air gap permeance, φ_{dj} is the phase of the j^{th} harmonic permeance of dynamic eccentricity, l=1, 2, …, n, j=1, 2, …, n.

Under the ITSC fault conditions, the magnetic flux density of the air gap generated by the k^{th} harmonic excitation magnetic potential is as follows,

$$\begin{aligned}B_k(\theta_r)&=F(\theta_r)\left(\frac{\lambda_0}{2}+\sum_{l=1,2,3,\cdots,n}\lambda_{2l}\cos 2lp\theta_r\right)\\&=\left\{\sum_{k=1,3,5,\cdots,n}F_k\cos(kp\theta_r)-\sum_{k=1,2,3,\cdots,n}\left[F_{k_1}\cos(k\theta_r)+F_{k_2}\sin(k\theta_r)\right]\right\}\\&\times\left(\frac{\lambda_0}{2}+\sum_{l=1,2,3,\cdots,n}\lambda_{2l}\cos 2lp\theta_r\right)\end{aligned} \tag{9}$$

According to equation (9), after the faulty, the k/p^{th} harmonics will appear in the main magnetic field. Therefore, the key to the ITSC of rotor winding detection based on magnetic field characteristics is to extract the k/p^{th} harmonics.

The j^{th}(j=1, 2, …, n)harmonic of air gap permeance generated by rotor dynamic eccentricity can be expressed as $\lambda_j\cos j(\theta_r+\varphi_{dj})$. The magnetic flux density generated by the k^{th}(k=1, 2, …, n) harmonic magnetic potential through the permeance modulation is as follows,

$$\begin{aligned}B(\theta_r)&=\sum_k F_k\cos(kp\theta_r)\times\sum_j\lambda_j\cos j(\theta_r+\varphi_{dj})\\&=\frac{F_k\lambda_j}{2}\sum_k\sum_j\left\{\begin{matrix}\cos\left[\theta_r(kp+j)+j\varphi_{dj}\right]\\+\cos\left[\theta_r(kp-j)-j\varphi_{dj}\right]\end{matrix}\right\}\end{aligned} \tag{10}$$

From the equation (10), it can be seen that after the rotor dynamic eccentricity fault, $(kp-j)/p^{th}$ and $(kp+j)/p^{th}$ harmonics appear in the air gap, where k=1, 3, 5…, n, j =1, 2, 3…, n. It can be seen that the frequency of the magnetic flux density is related to the number of poles, and contains fractional harmonics. The characteristic harmonics are near the two sides of the fundamental wave, the third harmonic and the fifth harmonic. The k/p^{th} harmonic content generated by the ITSC fault of the rotor winding is more complex, more abundant than the dynamic eccentricity, and the distribution is more dispersed.

III. Principle Analysis of Equivalent Coil

The stator core of the hydro-generator is made of silicon steel sheets. Cross-core screws are usually used to compress and fix the silicon steel sheets firmly in the axial direction. These cross-core screws are evenly arranged in the circumferential direction of the stator yoke. When connecting these screws with the stator core, the rotating magnetic field will form a strong circulating current between these screws, leading to a serious demagnetization. In this case, the iron core will be burnt under the iron core conduction effect. To avoid this, an insulation layer is provided between the screws and the core. At the end region of the stator core, the cross-core screw is also insulated from the end pressure plate, so the circulating current can be effectively avoided.

During operation, the cross-core screws cut the magnetic lines of force and induce a higher voltage at the ends of one screw, similar to a single bar in a stator slot. In order to get the characteristics of the ITSC magnetic field, the two ends on one side of any two cross-core screws are connected together to form an equipotential point, and the other side connected to the data acquisition instrument is used as output terminal, as shown in Fig. 2.

Assume that the m cross-core screws are evenly arranged in the circumferential direction of a hydro-generator (usually the same as the number of stator slots), the spatial mechanical angle between two adjacent screws can be expressed as,

$$\alpha=\frac{360^\circ}{m} \tag{13}$$

where, m represents the number of cross-core screws.

Any two screws are connected to form an equivalent coil, as shown in Fig. 2. Assume that the space mechanical angle between the two screws is $n\alpha$(n is the number of intervals between the two screws). For any ν harmonic magnetic field (for a $2p$-pole hydro-generator, it is actually ν/p^{th} harmonics, but we mainly analyze the harmonics of the magnetic potential under fault conditions, so the number of magnetic poles may not be considered), the distance between the two screws is $\nu n\alpha$(space electrical angle). Therefore, the output voltage of the coil can be expressed as,

$$\begin{aligned}E_\nu&=4.44\nu f\Phi_\nu\sin\frac{\nu n\alpha}{2}\\&=4.44\nu f\Phi_\nu\sin\frac{\nu n\times 180^\circ}{m}\end{aligned} \tag{14}$$

where, f is the mechanical rotation frequency of the generator, and Φ_ν is the effective value of the coil magnetic flux when the coil pitch is equal to the polar distance of the ν^{th} harmonic magnetic field.

According to equation (14), its ability to reflect the ν^{th}

harmonic varies with the coil pitch, so in this subsection we aim to analyze the influence of different pitches on the results.

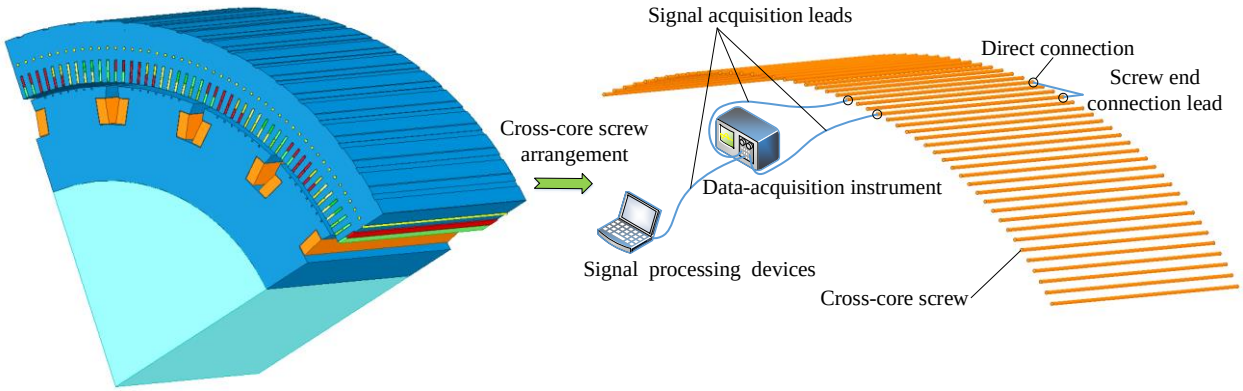

Fig.2. Schematic of a magnetic field detection coil consisting of two cross-core screws.

The selection of the coil pitch in Fig. 2 depends on the harmonics to be collected and the signal acquisition needs. For a 2*p* pole hydro-generator, the v/p^{th} harmonics are the fault characteristics to be collected. The selection of the coil pitch should ensure that one or more characteristic harmonics can be effectively collected, and the output voltage should be in the range that can be acquired directly by the instrument without transformer step-down.

IV. Finite Element Simulation

An SAV 620/27518 hydro-generator was taken as the research object. The basic parameters are listed in Table I. The corresponding finite element simulation model was built, as shown in Fig. 3.

First, the short circuit turn numbers of the faulty magnetic pole windings are set to 5, 10 and 15 respectively(total number of magnetic pole turns are 39), it can also be expressed as 12.8%ITSC, 25.6%ITSC and 38.4%ITSC. This is used to reflect the fault degree. In the paper, the stator slot number of the hydro-generator was the same with the number of cross-core screws, and both are 216. The generator pole number was 18, so the polar distance was expressed by the screw spacing, that is, 216/18=12. Therefore, we tried to change the pitch of the equivalent coil from the fractional multiple of the polar distance to integral multiple of polar distance and observe the harmonic contents in the induced voltages.

TABLE I
BASIC PARAMETER OF HYDRO-GENERATOR

Parameter	Value	Parameter	Value
Rated capacity /MVA	334	Rated voltage /kV	18±5%
Rated current /kA	10.71	Rated excitation current /A	1712
Air-gap length /mm	39.5	No-load excitation current /A	934.6
Number of stator slots	216	Number of phases	3
Number of rotor pole pairs	9	Number of magnetic poles	18
Number of cross-core screws	216	Rated speed (r/min)	333.3

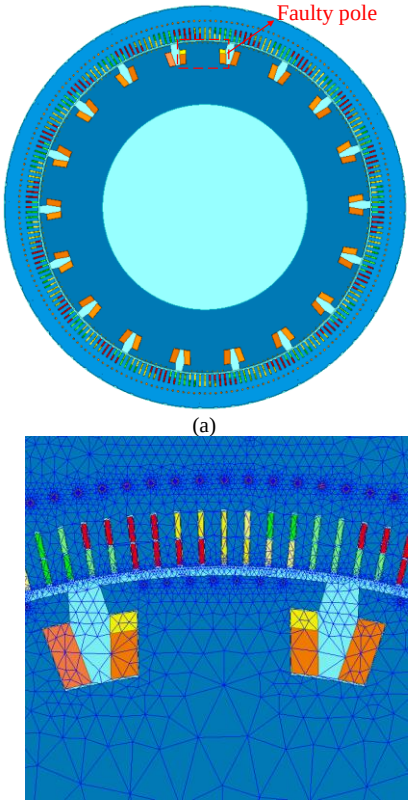

Fig. 3. Finite element model of the hydro-generator: (a) 2D model of the generator. (b) Model meshing.

Firstly, two adjacent screws were formed into an equivalent coil, that is, the pitch equaled one. The induced voltage of the equivalent coil was obtained by simulation, as shown in Fig. 4. It can be seen that when the faulty pole swept through the equivalent coil, the induced voltage was significantly reduced. There was no significant change in the induced voltage of the equivalent coil in other periods. Therefore, it can be concluded that the ITSC fault of the hydro-generator rotor winding can be determined by the change of the induced voltage of the equivalent coil, which is consistent with the theoretical analysis result. The Fourier decomposition of the induced voltage was carried out as shown in Fig. 4(b) and 4(d). To better display the amplitude of the harmonic, the waveform was locally amplified, so the amplitude of the fundamental

wave will not be fully presented, similarly hereinafter. It can be seen that after ITSC occurs, the voltage contains 1/9th(5.9Hz), 2/9th(11.1Hz), 1/3th(16.7Hz), 4/9th(22.2Hz) and other fractional harmonics, and the harmonic amplitude increases with the short-circuit turns. These simulation results are in good agreement those obtained by equation (9), which also verifies our method in detection ITSC fault of hydro-generators rotor winding.

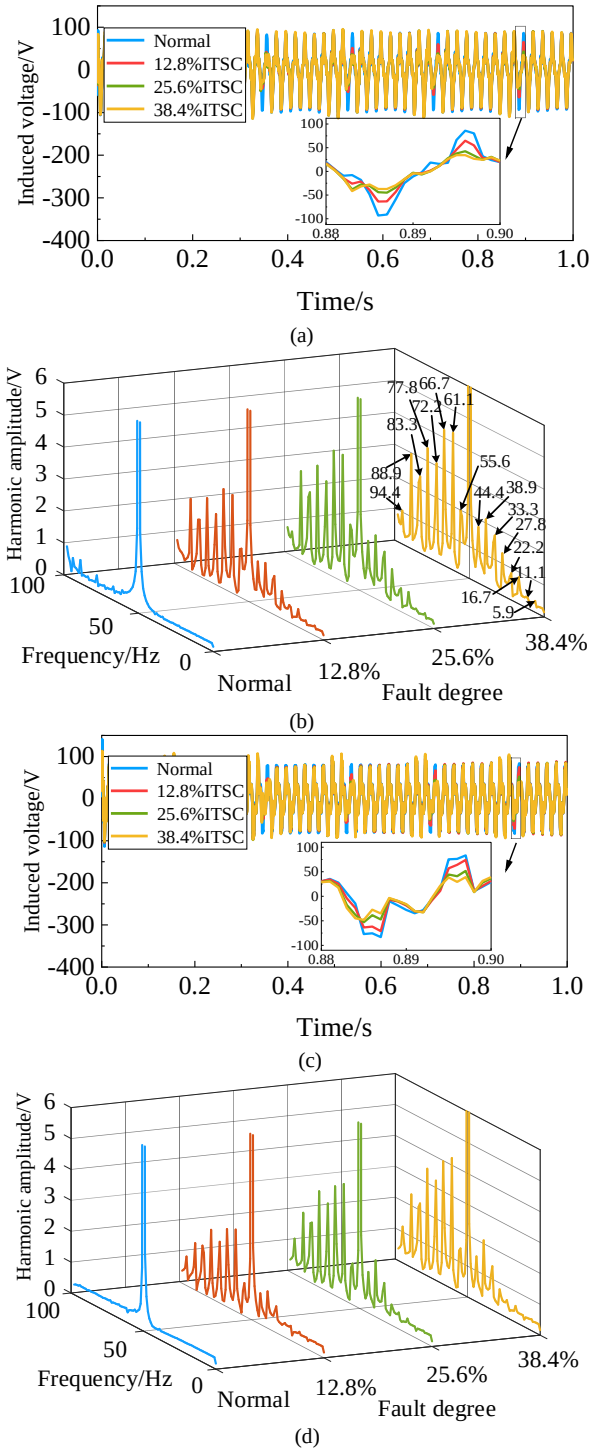

Fig. 4. Induced voltage of hydro-generator when coil pitch is one: (a) Time domain spectrum under no-load condition. (b) Frequency spectrum under no-load condition. (c) Time domain spectrum under on-load condition. (d) Frequency spectrum under on-load condition.

Next, The coil pitch was set to three and five respectively. The induced voltages of the equivalent coils are shown in Fig. 5 and Fig. 6. In the spectrum diagrams, there were 1/9th, 2/9th, 1/3th, 4/9th and other fractional harmonics, and these harmonic amplitudes increased with the increase of the fault degree. It can be seen that when the pitch of the equivalent coil was a fraction of generator polar distance, the ITSC fault can be accurately determined by the change of the induced voltage harmonics.

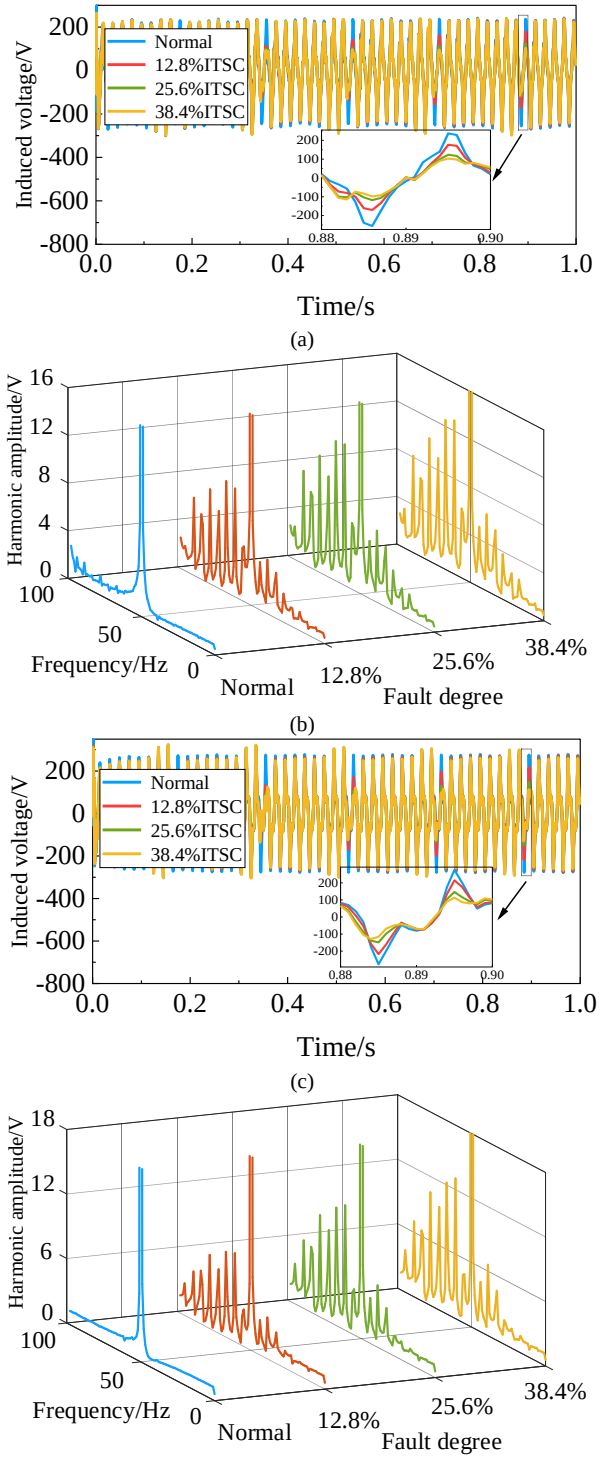

Fig. 5. Induced voltage of hydro-generator when coil pitch is three: (a) Time domain spectrum under no-load condition. (b) Frequency spectrum under no-load condition. (c) Time domain spectrum under on-load condition. (d) Frequency spectrum under on-load condition.

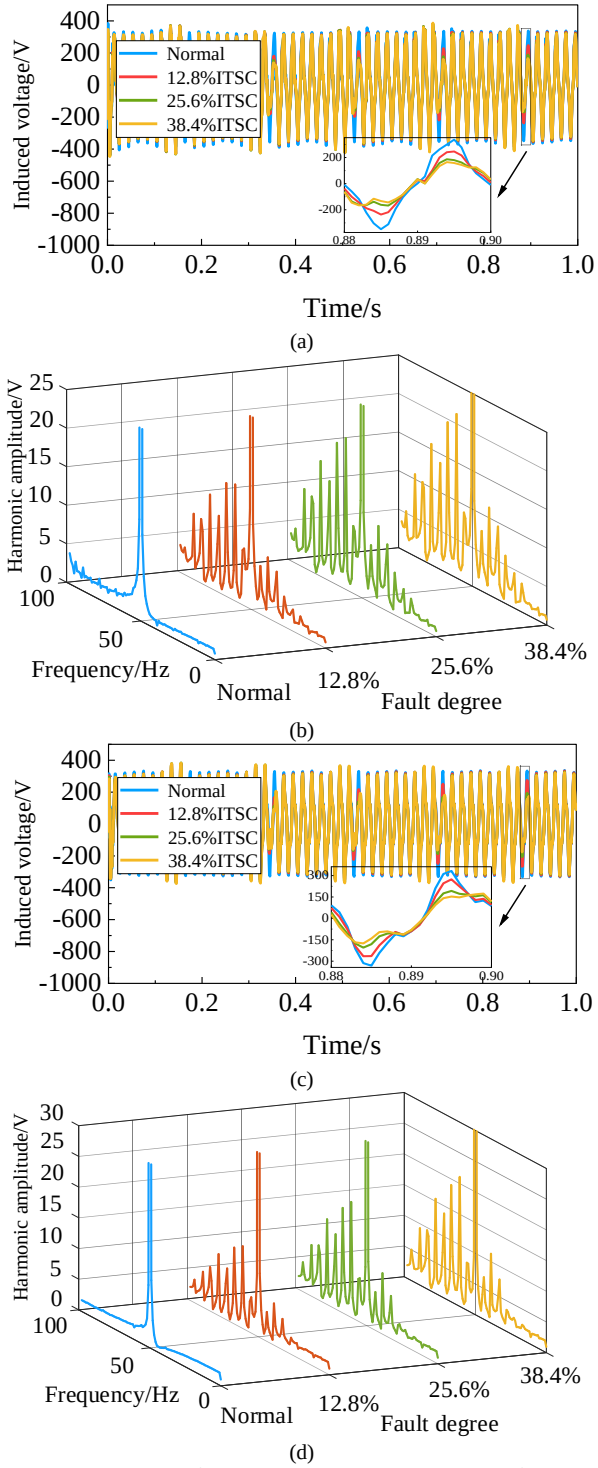

Fig. 6. Induced voltage of hydro-generator when coil pitch is five: (a) Time domain spectrum under no-load condition. (b) Frequency spectrum under no-load condition. (c) Time domain spectrum under on-load condition. (d) Frequency spectrum under on-load condition.

Next, we simulated the induced voltage in a coil whose screw distance is an integral multiple of the polar distance. To avoid excessive output coil voltage, we selected the pitch with integral multiple of the polar distance.Firstly, the pitch was set to 24, twice the polar distance. The induced voltage of the equivalent coil is shown in Fig. 7. It can be seen that when the faulty pole swept through the equivalent coil, the attenuation degree of the induced voltage was smaller compared with that of the equivalent coil with fractional multiple. There was no obvious change in the induced voltage in other periods. The spectrum of the induced voltage is shown in Fig. 7(b) and 7(d). It can be seen that after ITSC, the voltage contains $1/9^{th}$, $2/9^{th}$, $1/3^{th}$, $4/9^{th}$ and other fractional harmonics, and the harmonic amplitude increases with the fault degree. The ITSC fault of rotor winding can be accurately determined according to the fractional harmonic voltage of the equivalent coil.

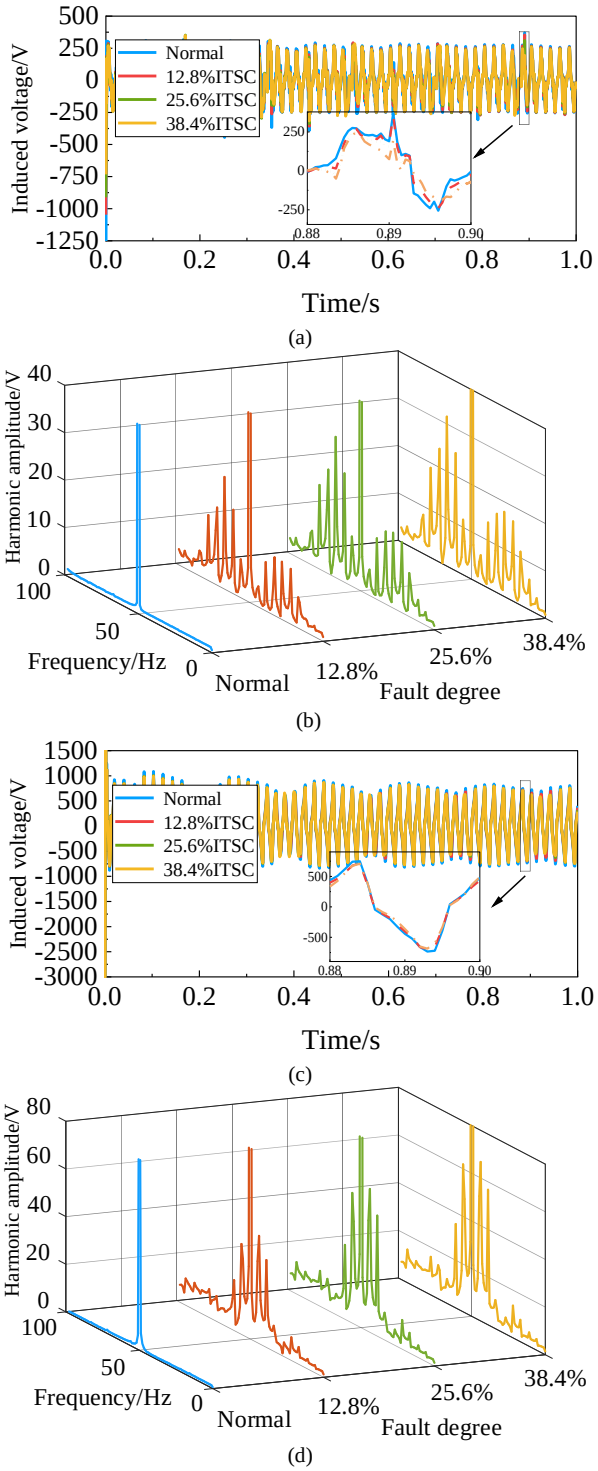

Fig. 7. Induced voltage when the pitch is twice the polar distance: (a) Time domain spectrum under no-load condition. (b) Frequency spectrum under no-load condition. (c) Time domain spectrum under on-load condition. (d) Frequency spectrum under on-load condition.

Then we changed the pitch of the equivalent coil and chose two screws with its pitch four times and six times the polar distance. The pitch was set to 48 and 72 respectively. The variation of the induced voltage and the harmonic frequency can be observed in Fig. 8 and Fig. 9.

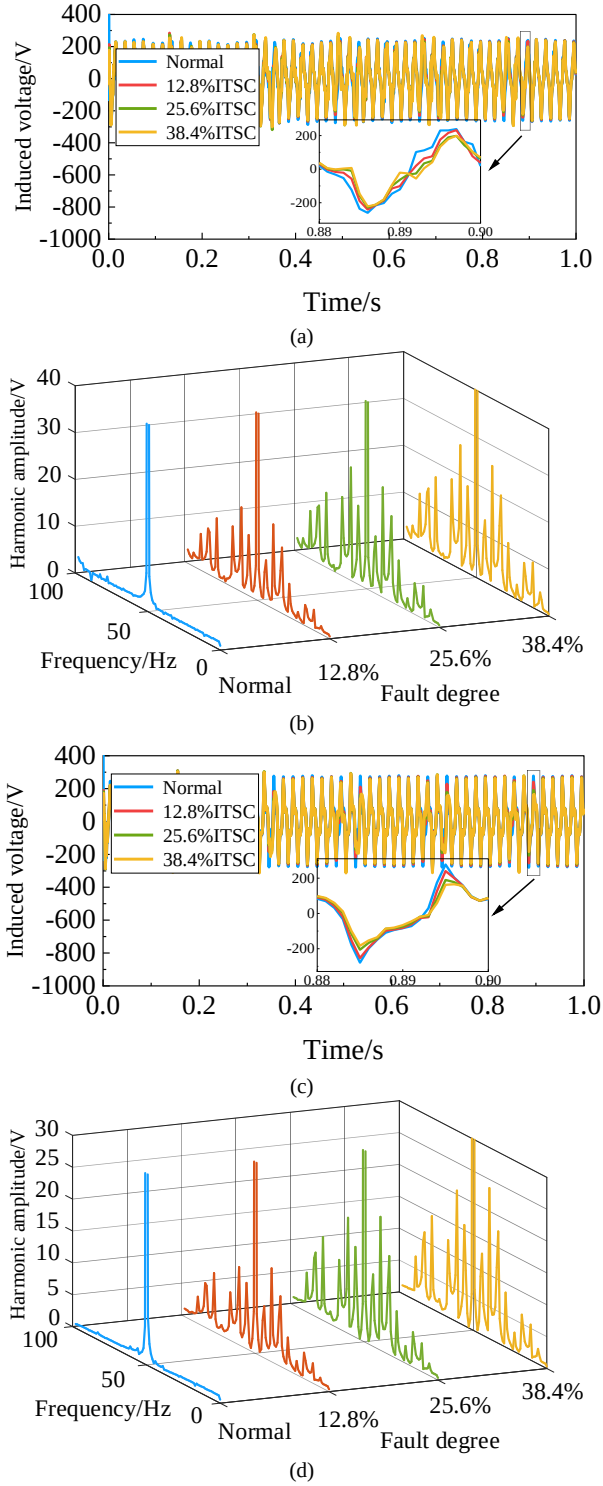

Fig. 8. Induced voltage when the pitch is four times the polar distance: (a) Time domain spectrum under no-load condition. (b) Frequency spectrum under no-load condition. (c) Time domain spectrum under on-load condition. (d) Frequency spectrum under on-load condition.

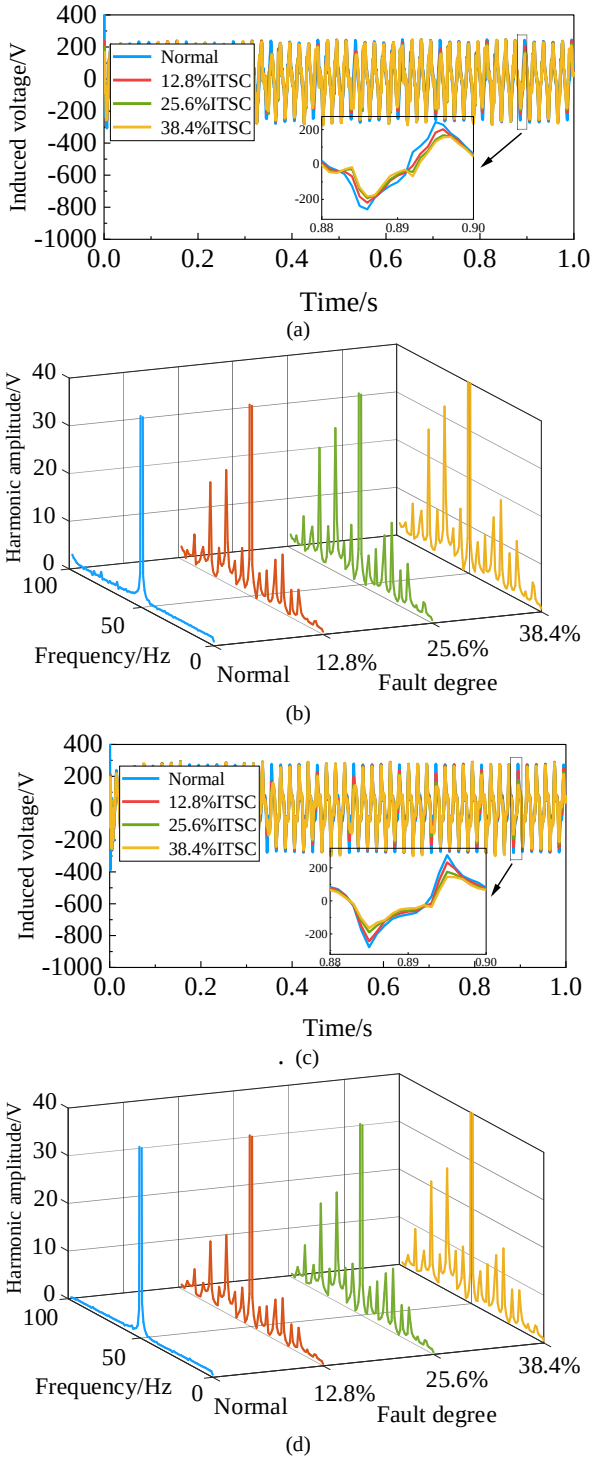

Fig. 9. Induced voltage when the pitch is six times the polar distance: (a) Time domain spectrum under no-load condition. (b) Frequency spectrum under no-load condition. (c) Time domain spectrum under on-load condition. (d) Frequency spectrum under on-load condition.

From Fig. 8 and Fig. 9, it can be seen that the $1/9^{th}$, $2/9^{th}$, $1/3^{th}$, $4/9^{th}$ and other fractional harmonics also appeared in the spectrum. It proves that the equivalent coil with integral multiple of the generator polar distance can also effectively detect the ITSC fault of the hydro-generator rotor winding. It can be seen that the spectrum amplitude increases with the fault degree. As the ITSC fault can be determined according to the characteristic harmonics, the adoption of the pitch of

integral multiple of polar distances has good detection effect.

V. Fault Test Simulation

A. Introduction of Test Platform

In order to verify the effectiveness of the detection method, the paper builds an test platform as shown in Fig. 10. The platform uses a DC motor as the prime mover to drive a 4-pole synchronous generator with a rated capacity of 2kW. The parameters are shown in Table II. Before the test, the structure of the generator was modified as follows:

The original stator part is pressed out of the casing with a press, and the CAD drawings of the stator core are mapped. A new stator core is processed according to the drawings, and 36 round holes with a diameter of 3mm are uniformly drilled on the stator yoke, as shown in Fig. 11(a). A new winding is embedded in the core slot, which is the same as the original stator winding, as shown in Fig. 11(b). The insulated wire is penetrated into the core hole of the stator to simulate cross-core screws of the large generator. The detection coils with pitches of 1, 3 and 18 are formed by the connection of the wire. The coil is extracted from the excitation side of the generator and connected to the data acquisition instrument. As shown in Fig. 11(c), the sampling frequency of the acquisition instrument is 10 kHz.

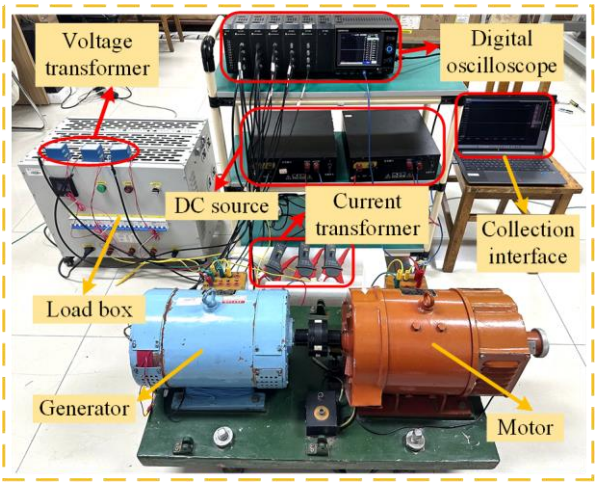

Fig. 10. Overall arrangement of the test.

TABLE II
MAIN PARAMETERS OF SYNCHRONOUS GENERATOR

Parameter	Value	Parameter	Value
Rated capacity /(kW)	2	Rated excitation current /A	3.54
Rated capacity /(kVA)	2.5	Rated power factor	0.8
Rated voltage /V	400	Parallel branches	2
Number of stator slots	36	Rated frequency /Hz	50
Stator inner diameter /mm	75	Rotor outer diameter /mm	74.5
Rated speed (r/min)	1500	Number of magnetic poles	4
Number of turns	150		

The test simulated the no-load and load conditions of the generator. Before the test, the excitation winding with a certain number of turns of a magnetic pole of the rotor is cut off, and the remaining winding is re-welded to realize the simulation of the rotor ITSC fault. The normal rotor winding and the fault winding are shown in Fig. 11(d).

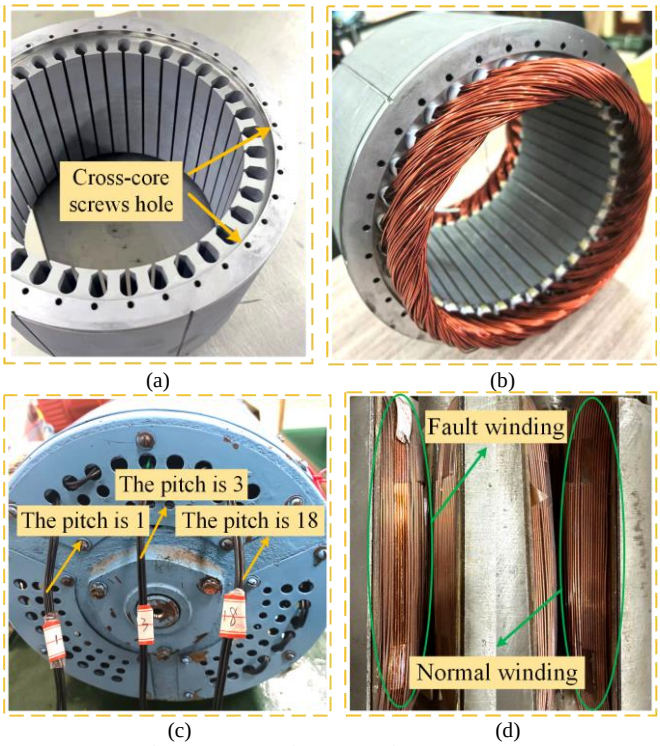

Fig. 11. Details of structural transformation of synchronous generator: (a) Screw hole position. (b) Stator winding. (c) Coil extraction position. (d) Comparison of normal and fault windings.

B. Test data analysis

The stator voltage and current of the unit under normal no-load and load conditions are shown in Fig. 12.

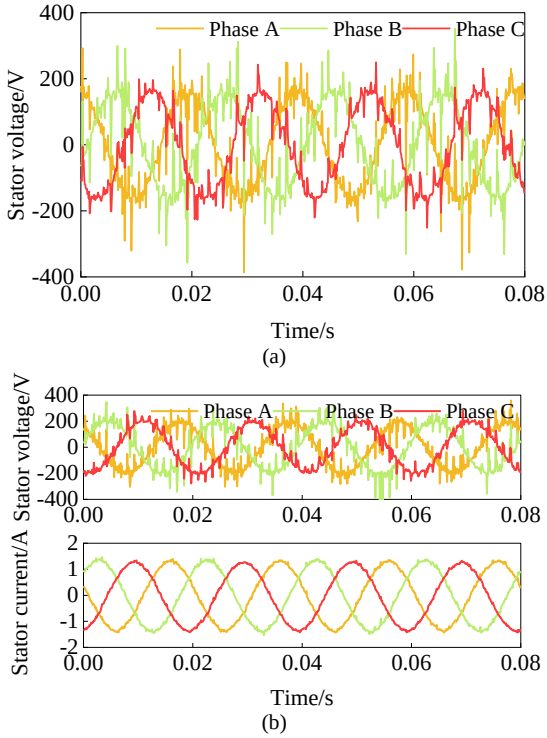

Fig. 12. Stator voltage and current: (a) No-load stator voltages. (b) Load stator voltage and current.

There are obvious harmonics in the stator voltage, which is after the transformation of the experimental generator, the stator adopts a straight slot structure (originally an oblique 1-slot structure). As a result, the stator voltage has obvious tooth harmonics. The harmonic frequency is related to the number of teeth Q/p under each pair of magnetic poles.

When the pitch of the equivalent coil is 1, 3 (fractional multiple of the polar distance) and 18 (integer multiple of the polar distance), the induced voltage of the detection coil is shown in Fig. 13-15. It can be seen that the induced voltage amplitude measured when the pitch of the detection coil is 18 (integer multiple of the polar distance) is much smaller than that measured when the pitch is 1 and 3 (fractional multiple of the polar distance). The amplitude of the induced voltage fractional harmonic of the detection coil is shown in Fig. 16.

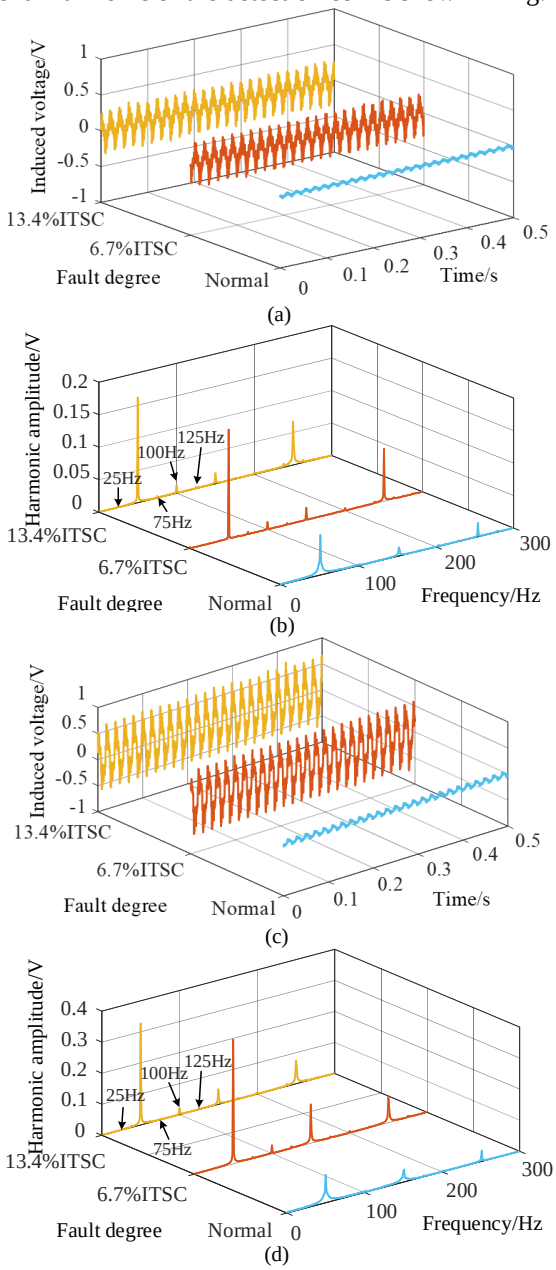

Fig. 13. Induced voltage when the pitch is 1: (a) Time domain spectrum under no-load condition. (b) Frequency spectrum under no-load condition. (c) Time domain spectrum under on-load condition. (d) Frequency spectrum under on-load condition.

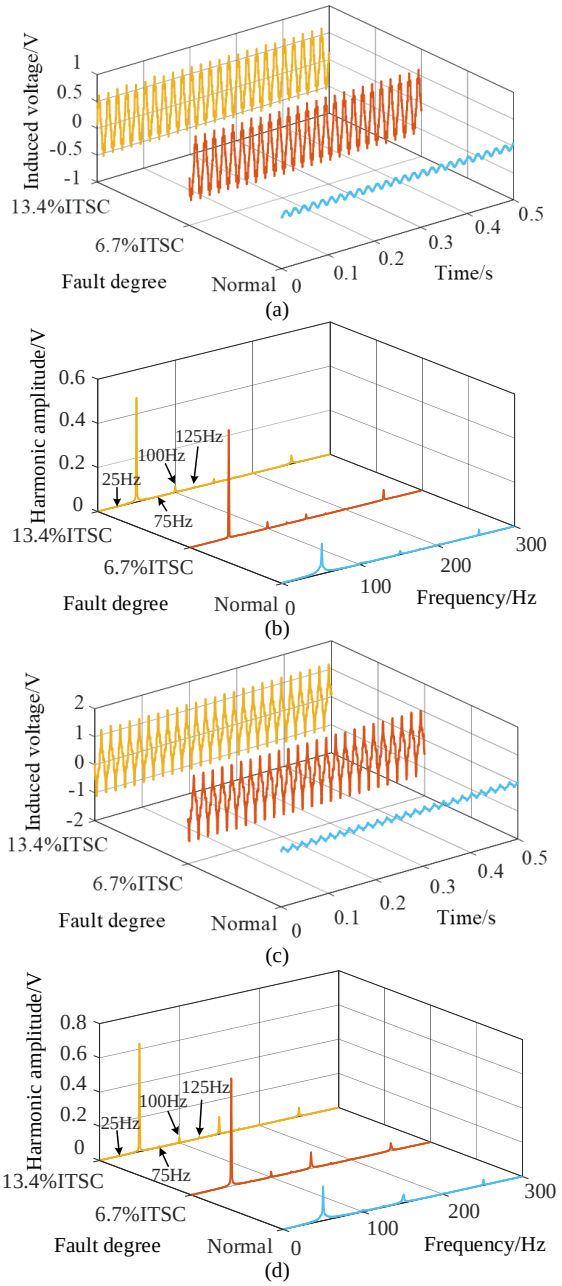

Fig. 14. Induced voltage when the pitch is 3: (a) Time domain spectrum under no-load condition. (b) Frequency spectrum under no-load condition. (c) Time domain spectrum under on-load condition. (d) Frequency spectrum under on-load condition.

It can be seen that when two cross-core screws form an equal value coil, after the ITSC fault of the rotor, the induced voltage of the coil increases under no-load and load conditions. When the degree of short circuit increases, the induced voltage of the coil does not change significantly. The fractional harmonics of 25Hz($1/2^{th}$), 75Hz ($3/2^{th}$), 100Hz (2^{th}) and 125Hz ($5/2^{th}$) in the induced voltage amplitude of the detection coil increase to a certain extent, and the amplitude of the fractional harmonic is greater than that of the even times when the pitch is the fractional times of the polar distance. It can be seen that the inter-turn short circuit fault of the rotor winding can be effectively detected when the detection coil is selected at different pitches. Under normal conditions of the unit, the coil induction voltage also contains a small amount of fractional

harmonics, which indicates that there is a certain error in the prototype manufacturing stage, which is difficult to avoid for a 2kW small unit.

It can also be seen from the diagram that for the 4-pole generator, the influence of the fault degree on the harmonic amplitude is not significant, indicating that the equivalent coil can detect ITSC of rotor winding fault by observing the change of the fractional harmonic amplitude, but it does not have the ability to reflect the degree of ITSC fault of the rotor of the 4-pole generator.

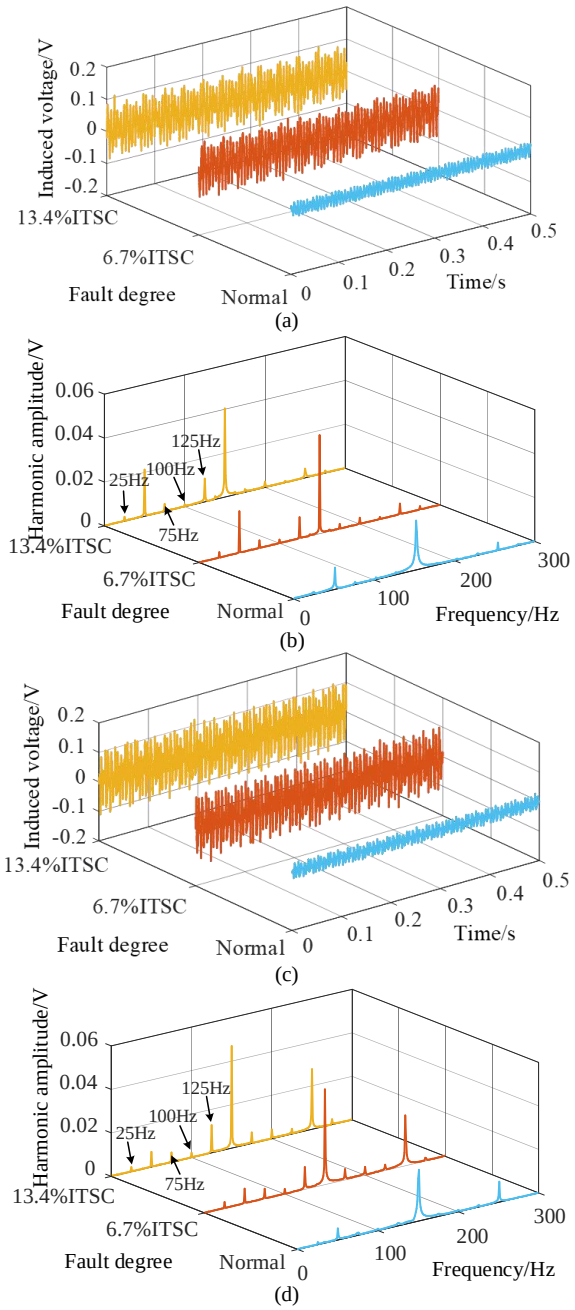

Fig. 15. Induced voltage when the pitch is 18: (a) Time domain spectrum under no-load condition. (b) Frequency spectrum under no-load condition. (c) Time domain spectrum under on-load condition. (d) Frequency spectrum under on-load condition.

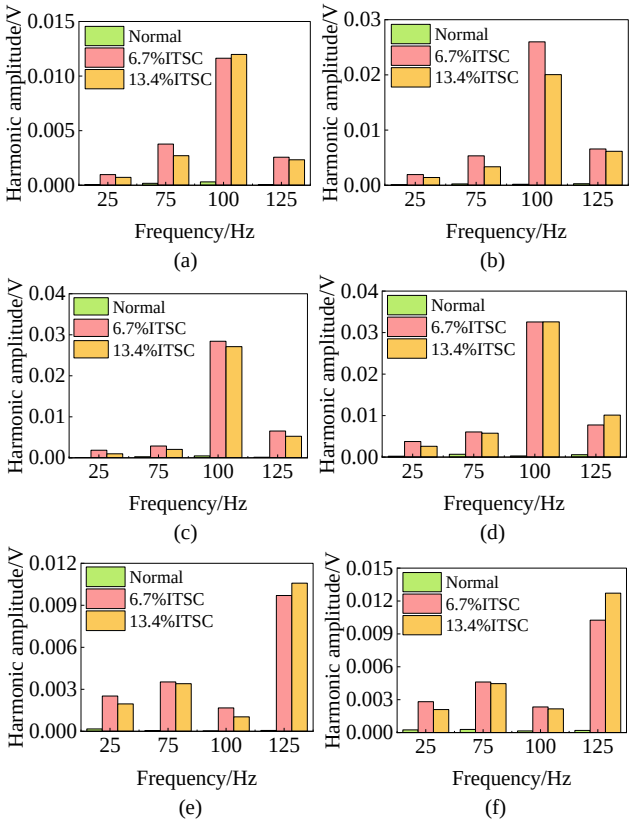

Fig. 16. The amplitude of fractional harmonic: (a) The pitch is 1 in no-load. (b) The pitch is 1 in on-load. (c) The pitch is 3 in no-load. (d) The pitch is 3 in on-load. (e) The pitch is 18 in no-load. (f) The pitch is 18 in on-load.

VI. Conclusion

In this paper, a new on-line diagnosis method for ITSC of hydro-generator rotor windings using flexible pitch equivalent coil is proposed. The induced voltage characteristic spectrum is obtained by simulation and fault experiment, the following conclusions are drawn:

(1) The main magnetic field inside the synchronous generator can be measured by the equivalent coil composed of two cross-core screws with different pitches. In addition to the normal odd harmonics, the induced voltage of the detection coil also contains fractional harmonics such as v/p (v= 1,2,3,..., n), which can reflect the asymmetry of the generator magnetic field caused by the ITSC of the rotor winding effectively.

(2) For multi-pole hydro-generators, the pitch of the equivalent coil can be fractional or integer times of the polar distance. It can be changed according to the number of the generator's cross-core screws. No matter what pitch is used, the ITSC fault of the rotor winding can be accurately determined.

(3) After the proposed method accurately detects the fault, it can propose a targeted fault handling scheme, which has important practical significance for reducing the vibration hazard of the unit and improving the operation safety. The proposed method is applicable to both static excitation generators and rotating excitation generators. It has the advantages of convenient implementation, little influence on the normal operation of generator and no hidden danger.

REFERENCES

[1] X. Yuan, Y. He, M. Liu, H.Wang et al., "Impact of the field winding interturn short-circuit position on rotor vibration properties in synchronous generators", *Math. Probl. Eng.*, vol. 2021, no. pt.49, pp. 1-11, Nov. 2021.

[2] I. Sadeghi, H. Ehya, J. Faiz et al., "Online condition monitoring of large synchronous generator under short circuit fault-A review, " *2018 IEEE International Conference on Industrial Technology (ICIT)*, pp. 1843-1848, 2018.

[3] H. Ehya, J. Faiz, "Introduction to different types of faults in synchronous generators", *Electromagnetic Analysis and Condition Monitoring of Synchronous Generators*, pp. 89-107, 2023.

[4] J. Yun, S. Park, C. Yang et al., "Comprehensive monitoring of field winding short circuits for salient pole synchronous motors, " *IEEE Trans. Energy Convers.*, vol. 34, no. 3, pp. 1686-1694, Sept. 2019.

[5] J. Hang, X. Shu, S. Ding et al., "Robust open-circuit fault diagnosis for PMSM drives using wavelet convolutional neural network with small samples of normalized current vector trajectory graph," *IEEE Trans. Ind. Electron.*, vol. 70, no. 8, pp. 7653-7663, Aug. 2023.

[6] Y. Li, H. Li, H. Zhao, "The new criterion on inter turn short-circuit fault diagnose ofsteam turbine generator rotor windings, " *Proceedings of the CSEE*, no. 6, pp. 112-116, 169, 2003.

[7] Y. Li, Y. Sun, L. Wang et al, "The criterion on inter-turn short circuit fault diagnose of steam turbine generator rotor windings," *2007 International Conference on Electrical Machines and Systems*, pp. 1050-1054, Oct.8-11, 2007.

[8] Y. Wu, Y. Li, "Diagnosis of rotor winding interturn short-circuit in turbine generators using virtual power," *IEEE Trans. Energy Convers.*, vol. 30, no. 1, pp. 183-188, Mar. 2015.

[9] Y. Wu, Y. Li, "Diagnosis of short circuit faults within turbogenerator excitation winding based on the expected electromotive force method," *IEEE Trans. Energy Convers.*, vol. 31, no. 2, pp. 706-713, Jun. 2016.

[10] G. Qin, X. Wang, Y. Jin et al, "Online monitoring of inter-turn short circuit fault of field winding in large turbo-generator" *2021 24th International Conference on Electrical Machines and Systems (ICEMS)*, Gyeongju, Korea, pp. 1619-1623, Dec. 2021.

[11] Y. Sun, X. Yu, K. Wei et al, "A new type of search coil for detecting inter-turn faults in synchronous machines, " *Proceedings of the CSEE*, vol. 34, no. 6, pp. 917-924, 2014.

[12] Y. Li, H. Li, H. Zhao et al, "Fault identification method of rotor inter turn short-circuit using stator winding detection," *2003 6th International Conference on Electrical Machines and Systems(ICEMS)*, Beijing, China, vol. 2, pp. 856-860, Nov. 2003.

[13] L. Hao, Y. Sun, A. Qiu et al., "Steady-state calculation and online monitoring of interturn short circuit of field windings in synchronous machines," *IEEE Trans. Energy Convers.*, vol. 27, no. 1, pp. 128-138, Mar. 2012.

[14] T. Plazenet, T. Boileau, C. Caironi et al, "An overview of shaft voltages and bearing currents in rotating machines," *2016 IEEE Industry Applications Society Annual Meeting*, pp. 1-8, Nov. 2016.

[15] Y. Wu, Y. Li, H. LI, "Diagnosis of non-salient pole synchronous generator rotor's t-ypical faults based on shaft voltage," *Transactions of China Electrotechnical Society*, Vol. 25, no.6, pp. 178-184, 2010.

[16] M. Duan, Z. Ou, C. Deng, "Analysis of shaft voltage in rotor permanent magnet synchronous motor system for traction," *2020 15th IEEE Conference on Industrial Electronics and Applications (ICIEA)*, pp. 1908-1911, Nov. 2020.

[17] T. Plazenet, T. Boileau, C. Caironi et al, "A comprehensive study on shaft voltages and bearing currents in rotating machines," *IEEE Trans. Ind. Appl.*, vol. 54, no. 4, pp. 3749-3759, July-Aug. 2018.

[18] Y. Wu, Q. Ma, B. Cai et al, "A new on-line fault diagnosis method of inter-turn short circuit fault in rotor winding of hydro-generator," *Electric Machines and Control*, vol. 22, no. 11, pp. 19-25, 2018.

[19] H. Ehya, A. Nysveen, I. L. Groth et al, "Detailed magnetic field monitoring of short circuit defects of excitation winding in hydro-generator," *2020 International Conference on Electrical Machines (ICEM)*, 2020, pp. 2603-2609.

[20] H. Ehya, A. Nysveen, "Pattern recognition of interturn short circuit fault in a synchronous generator using magnetic flux," *IEEE Trans. Ind. Appl.*, vol. 57, no. 4, pp. 3573-3581, July-Aug. 2021.

[21] S. Afrandideh, M. E. Milasi, F. Haghjoo et al, "Turn to turn fault detection, discrimination, and faulty region identification in the stator and rotor windings of synchronous machines based on the rotational magnetic field distortion," *IEEE Trans. Energy Convers.*, vol. 35, no. 1, pp. 292-301, Mar. 2020.

[22] O. Kokoko, A. Merkhouf, A. Tounzi et al., "Detection of short circuits in the rotor field winding in large hydro-generator," *2018 13th International Conference on Electrical Machines (ICEM)*, Alexandroupoli, Greece, 2018, pp. 1815-1820.

[23] J. Yun, S. B. Lee, M. Šašić et al, "Reliable flux-Based detection of field winding failures for salient pole synchronous generators," *IEEE Trans. Energy Convers*, vol. 34, no. 3, pp. 1715-1718, Sept. 2019.

[24] S. Bernier, A. Merkhouf, K. Al-Haddad, "Stray flux and air gap flux experimental measurement and analysis in large hydro generators," *2023 IEEE Workshop on Electrical Machines Design, Control and Diagnosis (WEMDCD)*, Newcastle upon Tyne, United Kingdom, 2023, pp. 1-6.

[25] Y. Wu, Q. Ma, B. Cai, "Fault diagnosis of rotor winding inter-turn short circuit for sensorless synchronous generator through screw," *IET Electric Power Appl.*, Vol. 11, no. 8, pp.1475-1482, Jul. 2017.

[26] P. Qi, Y. Li, M. Ma et al, "Diagnosis of inter-turn short circuit in excitation winding of pumped storage unit based on frequency resolved circulation spectrum," *IET Electric Power Appl.*, Vol. 17, no. 1, Jan. 2023.

Yucai Wu was born in Qiqihaer, China, on March 6, 1982. He received his Ph.D. degree in electrical engineering from North China Electric Power University, Baoding, Hebei, China, in 2010.

He is currently an associate professor in the North China Electric Power University. His research interests include the analysis of generator vibration, shaft voltage, and the fault diagnosis of electrical machines.

Xuanjie Fan was born in Zhangjiakou, China, on January 21, 1998. He received the B.E. degree in electrical engineering from Hebei University of Technology, Tianjin, China in 2021.

He is currently working toward the M.S. degree at North China Electric Power University. His research interest is fault diagnosis of electrical equipment.

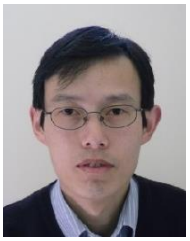

Lie Xu received the B.Sc. degree in mechatronics from Zhejiang University, Hangzhou, China, in 1993, and the Ph.D. degree in electrical engineering from the University of Sheffield, U.K., in 1999.

He is currently a Professor at the Department of Electronic and Electrical Engineering, University of Strathclyde, Glasgow, U.K. His research interests include power electronics, electrical machine fault diagnosis,and application of power electronics to power systems.

Weifu Lu was born in Hebei, China, in 1983. She received the B.E. degree from Qinghai University, Xining, Qinghai, China in 2006 and the Ph.D. degree from North China Electric Power University, Beijing, China in 2012.

She is currently a senior engineer with Pumped-storage Technological & Economic Research Institute, State Grid Xinyuan Company Ltd.. Her research interests include the structure selection and fault diagnosis of pumped storage generator-motor.

Cong Chen was born in Harbin, China, on May 22,1988. He received the M.Sc. degree in electrical engineering from Harbin University of Science and Technology, Heilongjiang, China, in 2014.

He is currently a senior engineer in the China Power Huachuang Electricity Technology Research Co., Ltd. His research interests include the Condition Maintenance of the Electrical Equipment, and the fault diagnosis of electrical machines.